Neural correlates of goal-directed and non–goal-directed movements

Naveen Sendhilnathan[a,b,c,d,e,f,1], Debaleena Basu[f], Michael E. Goldberg[b,c,d,e,g,h,1], Jeffrey D. Schall[i,j], and Aditya Murthy[f]

[a]Doctoral Program in Neurobiology and Behavior, Columbia University, New York, NY 10027; [b]Department of Neuroscience, Columbia University, New York, NY 10027; [c]Mahoney–Keck Center for Brain and Behavior Research, Columbia University, New York, NY 10027; [d]Zuckerman Mind Brain Behavior Institute, Columbia University, New York, NY 10027; [e]New York State Psychiatric Institute, New York, NY 10032; [f]Center for Neuroscience, Indian Institute of Science, Bangalore 560012, India; [g]Kavli Institute for Brain Science, Columbia University, New York, NY 10027; [h]Department of Neurology, Psychiatry, and Ophthalmology, Columbia University College of Physicians and Surgeons, New York, NY 10032; [i]Vanderbilt Vision Research Center, Department of Psychology, Vanderbilt University, Nashville, TN 37235; and [j]Center for Integrative and Cognitive Neuroscience, Department of Psychology, Vanderbilt University, Nashville, TN 37235

Contributed by Michael E. Goldberg, December 28, 2020 (sent for review May 5, 2020; reviewed by James W. Bisley and Lawrence H. Snyder)

What are the cortical neural correlates that distinguish goal-directed and non–goal-directed movements? We investigated this question in the monkey frontal eye field (FEF), which is implicated in voluntary control of saccades. Here, we compared FEF activity associated with goal-directed (G) saccades and non–goal-directed (nG) saccades made by the monkey. Although the FEF neurons discharged before these nG saccades, there were three major differences in the neural activity: First, the variability in spike rate across trials decreased only for G saccades. Second, the local field potential beta-band power decreased during G saccades but did not change during nG saccades. Third, the time from saccade direction selection to the saccade onset was significantly longer for G saccades compared with nG saccades. Overall, our results reveal unexpected differences in neural signatures for G versus nG saccades in a brain area that has been implicated selectively in voluntary control. Taken together, these data add critical constraints to the way we think about saccade generation in the brain.

saccade | frontal eye field | variability | beta

Many movements are goal-directed while others, such as fidgets, may not be. However, the differences between the neural mechanisms that control these different movements are poorly understood. The macaque frontal eye field (FEF) in particular has neurons that discharge before visually guided saccades and saccades made in total darkness such as learned saccades or memory-guided saccades (1) but not before spontaneous saccades in total darkness (2). Here, we discovered that when monkeys make saccades that have no obvious goal, in a lit environment, FEF movement and visuomovement neurons do, in fact, discharge. We asked if there were any differences in neural activities that distinguished non–goal-directed (nG) saccades from goal-directed (G) saccades.

We studied two characteristics of neural response not directly visible in the firing rate but which precede movements: a decrease in neural response variability (3) and a decrease in local field potential (LFP) beta oscillatory activity (4, 5). Previous studies have shown that decreases in response variability are correlated with attention (6), planning of saccades (3, 7, 8), the onset of a visual stimulus (3, 9), and the amount of expected reward (10), among other processes. Decreases in beta power have been correlated with motor preparation and inhibitory control (11, 12), among other processes (13). Nevertheless, despite these efforts, their roles in goal-directed versus non–goal-directed movement generation have not been studied.

Here, we studied simultaneously recorded neural spiking and LFP in the FEF in the primate frontal cortex and show evidence for differential cortical control for G and nG saccades: Although FEF saccade-related neurons do discharge before nG saccades, we found that for G saccades, but not for nG saccades, the variability in spike rate across trials decreased, and there was a concurrent reduction of LFP beta-band power. Furthermore, the time from saccade direction selection to saccade onset was significantly longer for G saccades compared with nG saccades.

Results

We trained two monkeys to perform a visually guided saccade task where the monkeys made saccades to locations instructed by a prior target presentation (14). We presented only one target in ∼30% of the trials, referred to as "no-step trials" (Fig. 1*A*), while in the remaining ∼70% of trials we presented two sequential targets, referred to as "step trials" (Fig. 1*B* and *SI Appendix*, Fig. S1*A*; see *Materials and Methods* for details) with varying target step delays (*SI Appendix*, Fig. S1*B*). The monkeys either made a single or two sequential visually guided saccades, respectively, to earn a liquid reward. We only analyzed correct trials in this study (*SI Appendix*, Fig. S1*C*).

In this study, we defined G saccades as those task-relevant, visually guided, reward-driven saccades that were instructed by a prior target presentation. We defined nG saccades as those saccades that were neither visually guided nor instructed by a prior target presentation and thus were task-irrelevant and not rewarded upon execution (these mostly occurred during the intertrial interval period). The monkeys first made either a single G saccade in the no-step trials or two sequential G saccades (G1 and G2) in the step trials, and then made an unpredictable number of random nG saccades before making a return (R) saccade to the spatial location of the fixation point at the center

Significance

Although the monkey frontal eye field is implicated in the voluntary control of saccades, we found that only for during goal-directed saccades the variability in spike rate across trials decreased and had a concurrent reduction of LFP beta-band power, and the neural activity increased earlier. These data indicate the presence of additional constraints and computations that distinguish goal-directed movements from non–goal-directed movements.

Author contributions: N.S. conceived the study; D.B. and A.M. designed the study; D.B. collected the data; N.S. analyzed the data; M.E.G. and A.M. supervised the analysis; and N.S., D.B., M.E.G., J.D.S., and A.M. contributed to writing the paper.

Reviewers: J.W.B., David Geffen School of Medicine at University of California, Los Angeles; and L.H.S., Washington University in St. Louis School of Medicine.

The authors declare no competing interest.

[1]To whom correspondence may be addressed. Email: ns3046@columbia.edu or meg2008@columbia.edu.

This article contains supporting information online at https://www.pnas.org/lookup/suppl/doi:10.1073/pnas.2006372118/-/DCSupplemental.

Published February 5, 2021.

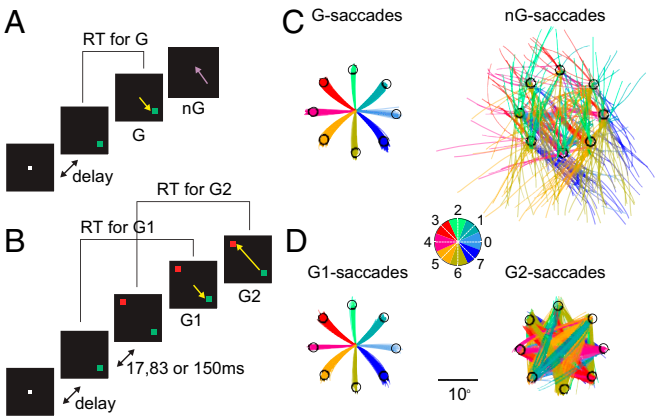

Fig. 1. Task and behavior. (*A*) Follow task: no-step trials. The monkeys fixated on a central white square fixation spot on a dark background. Following a variable time delay, a peripheral green target appeared and the monkeys made a single G saccade (yellow arrow) to this target location as soon as possible. The monkeys fixated on the target for 200 ms and then were free to move their eyes. Then, the monkeys often made (*A*) task-irrelevant nG saccade(s), shown in purple. (*B*) Follow task: step trials. The monkeys fixated on a central white square fixation spot on a dark background. Following a variable time delay, two peripheral targets (green and red) appeared sequentially with a delay between them and the monkeys made two sequential G saccades (yellow arrow) to these target locations as soon as possible. The monkeys fixated on the final target for 200 ms and then were free to move their eyes. (*C*) The saccade trajectories from two representative sessions for the G saccades (*Left*) and nG saccades (*Right*) in the no-step trials. The colors represent the vector direction to which the saccades were made, irrespective of the saccade's starting position (refer to the *Inset* for the colormap legend: If the center of the circle was the saccade's starting point, then the color of the saccade is the color represented by an outward-facing vector lying in that octant of the circle). (*D*) Same as *C*, but for the two sequential G saccades in step trials.

of the screen. We only analyzed the first pair of consecutive saccades in every trial: either G immediately followed by nG or R saccades in no-step trials (Fig. 1*C*) and two sequential G1 and G2 saccades in the same trial (Fig. 1*D*). Both types of sequential saccade pairs were matched in intersaccade intervals (*Materials and Methods* and *SI Appendix*, Fig. S1*E*).

We analyzed simultaneously recorded neural spiking activity and LFP from 34 visuomovement and 38 movement FEF neurons, using a previously reported dataset (4, 14), and excluded all visual neurons for our analyses (*SI Appendix*, Fig. S2). The FEF neurons fired with an increased discharge rate, from the baseline (B; −100 to 0 ms from the first target onset), during all these types of saccades (G, nG, G1, and G2). For saccades into the response field (RF), the peak neural activities for G saccades and nG saccades were significantly different (G: 49.24 ± 0.32 sp/s; nG: 38.74 ± 0.46 sp/s; $P < 0.001$, paired t test; Fig. 2*A*). However, the peak neural activity for G1 saccades and G2 saccades did not differ (G1: 53.32 ± 0.12 sp/s; G2: 52.12 ± 0.65 sp/s; $P = 0.13$, paired t test; Fig. 2*D*). The peak neural activities of nG saccades and G2 saccades were also significantly different (nG-G2: $P < 0.001$, paired t test).

We indexed the across-trial variability in firing rate during saccade preparation through the mean-matched Fano factor (FF), the variance in spike counts across trials divided by the mean across-trial firing rate (6). We controlled for the effect of changes in the mean firing rate on the FF by matching the average across-trial firing rate distributions across time bins using the algorithm developed by Churchland et al. (9) (*Materials and Methods*). Relative to the baseline, the FF decreased only for the G saccades (Fig. 2 *B* and *C*; B-G: $P < 0.001$, t test), while it did not significantly change for the nG saccades (Fig. 2 *B* and *C*; B-nG: $P = 0.74$, t test; G-nG: $P < 0.001$, t test). Although the neural activity was spatially tuned, the FF was untuned, consistent with previous reports (3, 7, 15). That is, the changes in FFs were similar for saccades into the RF and saccades out of the RF (aRF) for both types of saccades (G: RF-aRF: $P = 0.10$, rank-sum test; nG: RF-aRF: $P = 0.62$, rank-sum test) even though the firing rates were significantly different between RF and aRF by definition (G: RF-aRF: $P < 0.001$, paired t test; nG: RF-aRF: $P < 0.001$, paired t test). This suggests that the changes in the FF were not dependent on the direction of saccades.

One could hypothesize that the neural variability is suppressed only for the first saccade of a series of sequential saccades due to parallel processing (14) and hence the neural variability in the no-step trials only decreased for the first (G) saccade but not for the next (nG) saccade. To check if this is the case, we performed the same analyses on two sequential G saccades in the step trials (Fig. 2*D*) and found decreases in mean-matched FF (Fig. 2 *E* and *F*; G1: $P < 0.001$, t test; G2: $P < 0.001$, t test) for both saccades.

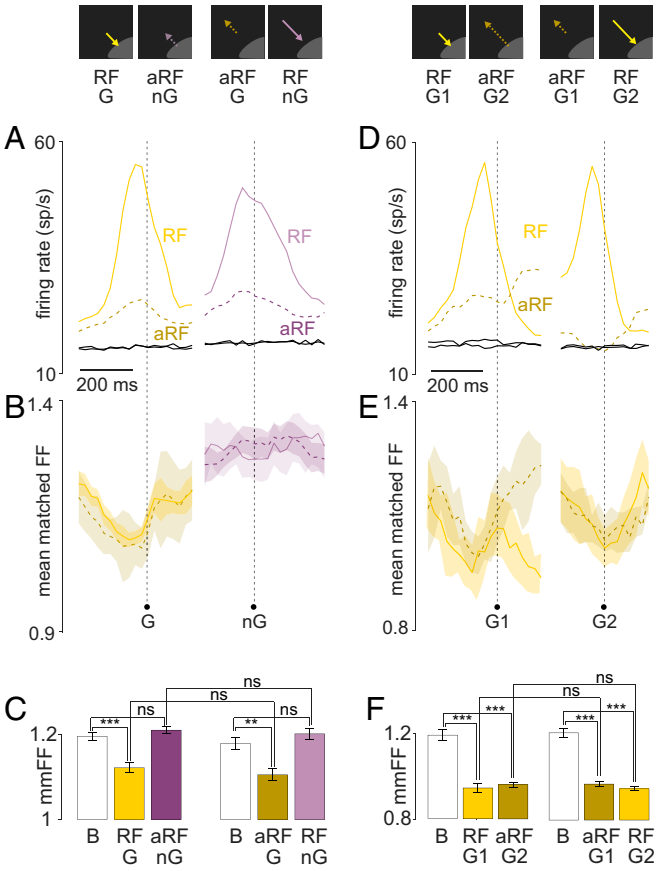

Fig. 2. Neural variability decreased only for G saccades. (*A*) Mean neural activity for G saccades into the RF (solid yellow line), G saccades into the aRF (broken brown line), nG saccades into the RF (solid violet line), and nG saccades into the aRF (broken purple line) in no-step trials. The corresponding mean-matched neural activities are shown in black. Signals (*Left*) were aligned to the start of G saccades and (*Right*) to the start of nG saccades (broken vertical lines). (*B*) Mean-matched FF for all the saccade types shown in *A*. (*C*) Quantitation of the mean-matched FF from *B*. Baseline (−100 to 0 ms from the first target onset). (*D*) Same as *A*, but for G1 and G2 saccades in step trials into the RF (yellow) and into the aRF (brown) conditions. Signals (*Left*) are aligned to the start of G1 saccades and (*Right*) to the start of G2 saccades (broken vertical lines). (*E*) Mean-matched FF for all the saccade types shown in *D*. (*F*) Quantitation of the mean-matched FF from *E*. ***$P <$ 0.001, **$P < 0.01$, *$P < 0.05$; ns, not significant, $P > 0.05$. Error bars indicate mean ± SEM.

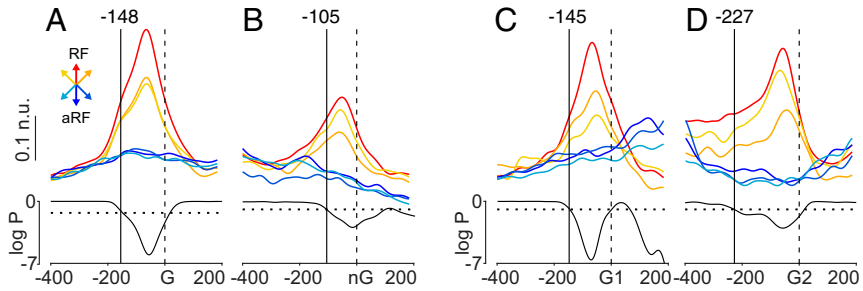

Fig. 3. Saccade plan specification was longer for G saccades than for nG saccades. (*A*) The mean neural activity (*Top*) and log-transformed *P* value from an ANOVA comparing the mean neural activities (*Bottom*) among all directions. The time at which this *P* value started to be significant (i.e., fell below the broken line indicating $P = 0.05$) was taken as the time of saccade plan specification (vertical black line). SPS was −148 ms for G saccades. (*B*) Same as *A*, but for nG saccades in no-step trials. SPS was −105 ms. (*C*) Same as *A*, but for G1 saccades in step trials. SPS was −144 ms. (*D*) Same as *A*, but for G2 saccades in step trials. SPS was −227 ms. n.u., normalized unit.

The FF for G2 saccades was significantly lower than the FF for nG saccades (G2-nG: $P < 0.001$, paired *t* test) while the FFs for G and G1 saccades were similar (G-G1: $P = 0.11$, paired *t* test). As a proof of concept, we found that the neural variability did not decrease for the third (nG) saccade after the two sequential G saccades in the step trials (*SI Appendix*, Fig. S3; $P = 0.23$, *t* test). We confirmed that the mean-matching process did not affect our conclusion since we obtained similar results using the raw Fano factor as well (*SI Appendix*, Fig. S4). Furthermore, R saccades, although not rewarded immediately, since they returned their gaze to the fixation point to initiate the next trial, could be construed as goal-directed. In support of this notion, they had lower FF (similar to G saccades) and were thus different from the FF of nG saccades (*SI Appendix*, Fig. S5). Taken together, we show that the across-trial variability in neural activity decreased for all saccades, except nG saccades.

Because the nG saccades were task-irrelevant and neither rewarded nor punished, they were heterogeneous in direction, amplitude, and velocity. Consequently, such variable kinematic and dynamic factors could confound our observation. However, we found no evidence suggesting that the FF for nG saccades that were matched in amplitude and velocity with G2 saccades was different from the FF for those nG saccades that differed from G2 saccades in amplitude or velocity ($P = 0.68$, rank-sum test; *SI Appendix*, Figs. S6 and S7). That is, within a class, the saccadic metrics did not affect the FF metrics. Furthermore, the time between the selection of saccade direction (see *Materials and Methods* for time of saccade plan specification; SPS) and the saccade onset was substantially longer for G saccades (−148 ms) compared with nG saccades (−105 ms; test; Fig. 3).

The LFP activity in the FEF during saccade planning reflects the local neural activity rather than an input to saccade planning (4) and the frequency component of the LFP provides complementary neural signatures that are not readily observable from just the fluctuations in the raw voltage amplitude. Specifically, beta-band (13 to 30 Hz) power has been linked to movement preparation and execution in several brain regions (13). Beta power is reduced before a voluntary movement and reaches a minimum around the time of movement execution, followed by a phasic rebound (4). Although average LFP activity decreased during both types of saccades in no-step trials (Fig. 4*A*; G: $P < 0.001$, rank-sum test; nG: $P < 0.001$, rank-sum test), the beta band decreased in power only during G saccades (4) but not for nG saccades (Fig. 4 *B* and *C*; G: $P < 0.001$, rank-sum test; nG: $P = 0.78$, rank-sum test). The beta power was not directionally tuned for either saccade type (Fig. 4*D*; nG: $P = 0.22$, ANOVA; G: $P = 0.33$, ANOVA). For step trials, the LFP activity decreased for both G1 and G2 saccades (Fig. 4*E*; G: $P < 0.001$, rank-sum test; G2: $P < 0.001$, rank-sum test), and the beta power was also suppressed for both saccades (Fig. 4 *F* and *G*; G1: $P < 0.001$, *t* test; G2: $P < 0.001$, *t* test). The beta power again was not directionally tuned for either type of saccade (Fig. 4*H*; G1: $P = 0.62$, ANOVA; G2: $P = 0.46$, ANOVA). Finally, the beta power was significantly different between nG and G2 saccades (nG-G2: $P < 0.001$, paired *t* test). Taken together, the activity of the beta band decreased only for G saccades and not for nG saccades.

Discussion

Although the FEF drives saccades, the neural signatures of G saccades significantly differed from nG saccades. We show three critical distinctions between the two types of movements: Only G

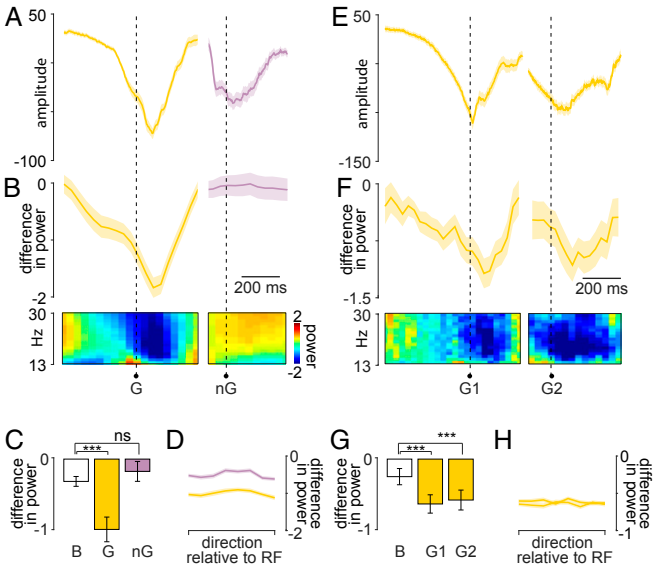

Fig. 4. LFP beta power decreased only for G saccades. (*A*) Mean LFP activity for G saccades (yellow) and nG saccades (purple) in no-step trials. Signals (*Left*) are aligned to the start of G saccades and (*Right*) to the start of nG saccades (broken vertical lines). (*B*, *Top*) Mean beta-band power (difference in power from baseline) for G saccades (yellow) and nG saccades (purple) in no-step trials. (*B*, *Bottom*) Spectrogram showing the beta-band modulation. (*C*) Quantitation from *B*. B-G: ***$P < 0.001$, rank-sum test; B-nG: $P = 0.77$, rank-sum test. (*D*) Lack of modulation of beta power with direction relative to the RF (center of the abscissa) for G saccades (yellow) and nG saccades (purple) in no-step trials. (*E*) Same as *A* but for two consecutive G saccades in the step trials. Signals (*Left*) are aligned to the start of G1 saccades and (*Right*) to the start of G2 saccades (broken vertical lines). (*F*) Same as *B* but for two consecutive G saccades in the step trials. (*G*) Quantitation from *F*. B-G1: ***$P < 0.001$, *t* test; B-G2: ***$P < 0.001$, *t* test. (*H*) Lack of modulation of beta power with direction for two consecutive G saccades in the step trials. Error bars indicate mean ± SEM.

saccades were accompanied by a decrease in across-trial variability, a decrease in LFP beta activity, and longer SPS latency. Here we discuss their implications.

A number of different factors have been associated with decreased across-trial variability: the appearance of a stimulus in the visual field, not necessarily in the RF of the neuron, in multiple visually responsive areas, including the V1, MT (mediotemporal area), LIP (lateral interparietal area), and FEF (3, 7, 9); motor planning for the target within or outside the RF (7, 8); saccade planning to stimuli in the inhibitory surround, which decreases with distance from the RF center (10); and attention to the stimulus in the RF (16). The first three of these factors are unlikely to be responsible for the decrease in FF during G but not nG saccades. It is true that there was a stimulus appearance in step trials that did not exist in no-step trials, but the decrease in the FF occurred near the beginning of the saccade, 400 ms after the appearance of the target, and the stimulus-induced FF occurred 50 ms after the appearance of the stimulus. The decrease in variability could not have been due to motor planning, because saccades occur, with similar kinematics, in both cases (*SI Appendix*, Fig. S6). Similarly, because no distracting stimulus appeared in either case, excitation of a putative inhibitory surround could not have caused the decrease in the G2 saccades.

However, the monkeys most likely attended to a spatial location in the G and R saccades but not in nG saccades. In addition, G and R saccades had higher firing rates compared with nG saccades, which is consistent with the fact that the responses of FEF neurons to attended targets are enhanced (17, 18). Since changes in the FF are also correlated with attention (19), we hypothesize that the lack of change in the FF for nG saccades could have been due to lack of attention, among other possibilities.

G saccades and R saccades had longer SPS times compared with nG saccades (Fig. 3 and *SI Appendix*, Fig. S5*C*). Several reasons can explain this observed difference. Since R saccades, which were not directly associated with a task-related reward per se, also had SPS latencies and FF patterns that resembled G saccades, we suggest that this pattern of responses maps onto their behavioral utility. Thus, shorter SPS latencies for nG saccades relative to saccade onset could possibly be interpreted as the likely absence of computations such as attention, and the release of inhibition, that help direct saccades to their goals, as opposed to reward per se. In terms of measurement, however, one can argue that larger trial-to-trial variability in neural activity for nG saccades (due to high FF) delays resolution of statistical differences in firing rates across directions, resulting in a shorter SPS for nG saccades. In contrast, G2 saccades had longer SPS times compared with G1 saccades (Fig. 3). This could be because of parallel processing since the planning of the G2 saccade begins before the G1 saccade is executed (14).

The amplitude of suppression of the LFP beta-band activity does not depend on motor parameters such as direction (20), speed (12), or the duration of the movement (21). Furthermore, artificially driving the motor cortex or the subthalamic nucleus at beta frequencies slows movement (11, 22). The mechanism of release of inhibition of the beta activity is currently unclear. Barbiturates such as thiopental are known to induce beta oscillations in the electroencephalogram of normal brain and have been used to identify abnormal brain tissue before epilepsy surgery (23, 24). The mechanism of action of barbiturates is γ-aminobutyric acid (GABA)-mediated inhibition of synaptic transmission. Furthermore, the GABAergic agonist benzodiazepine, which increases in the conductance of GABA-mediated currents, is also known to increase beta-band oscillations (25). The decrease of beta-band power induced by benzodiazepine can be modeled as a decrease in inhibitory current to the inhibitory interneurons but not a decrease in inhibitory currents to the excitatory pyramidal cells (25). These studies suggest that beta might represent a global movement suppression signal in the brain, which under release of inhibition might allow for movement preparation. Our data, which show that movement execution can occur in the absence of such a decrease in beta-band activity and presumably without a concomitant decrease in inhibition, argue against this interpretation. Instead, we interpret the differential pattern of beta as suggesting a selective role of cortical inhibition in the generation of goal-directed movements.

The question then arises if the FEF participates in driving nG saccades. The FEF movement cells project monosynaptically to the intermediate layers of the superior colliculus, which are critical for the generation of saccades and presumably drive most saccades. The superior colliculus movement cells fire before all saccades, including spontaneous saccades in total darkness, saccades which are not preceded by FEF activity. Nonetheless, it is difficult to postulate that the colliculus is not driven by the FEF for nG saccades, especially because the FEF activity has a longer presaccadic latency for nG saccades than the 30-ms minimal latency of the intermediate layers of the superior colliculus (26). If the FEF were to induce the superior colliculus to drive nG saccades in the absence of concomitant decreases in FF and beta, it could be that these non–spike-rate characteristics of neural activity have some function other than the transsynaptic transmission of information.

Materials and Methods

We performed all our analyses on previously published datasets of frontal eye field neurons (4, 7, 14). Please refer to those studies for full details. We briefly describe the experimental procedures and methods here.

Subjects. Two adult monkeys, Ja (male, *Macaca radiata*) and Gu (female, *Macaca mulatta*), were used for the experiments and were cared for in accordance with the Committee for the Purpose of Control and Supervision of Experiments of Animals, Government of India, and the Institutional Animal Ethics Committee of the Indian Institute of Science.

Behavioral Tasks.

Memory-Guided Saccade Task. We used this task (*SI Appendix*, Fig. S2*A*) to classify FEF cells into visual, visuomovement, and movement neurons (see below for visuomotor index) and to identify the response field of the neuron, the direction that elicited the maximum response before a saccade. Details of this task have been described in detail elsewhere (4). The monkeys were required to fixate on a central fixation point for a variable amount of time (~300 ms) at the start of the trial, following which a gray target appeared briefly at one of the eight equally spaced peripheral locations on an imaginary circle of radius 12°. The monkeys had to continue fixation on the central fixation point for a variable delay (1,000 ms ± 15% jitter, sampled from a uniform distribution), following which the fixation point disappeared (go signal), cueing the monkeys to make a goal-directed memory-guided saccade (MGS) to the remembered target location, following which the target briefly reappeared. On successful trials, the monkeys received a juice reward. The monkeys were required to maintain fixation on the target location for 200 ms after the end of the goal-directed saccade. After that there was a 1,000-ms period (500 ms until the end of the trial and 500 ms of intertrial interval) during which they often made none or several non–goal-directed saccades before returning back to the center of the screen in preparation for the next trial.

Follow Task. Details of this task have been described in detail elsewhere (14). We describe it briefly here. Each trial started with the appearance of a white central fixation point. The task was composed of two types of trials that were randomly interleaved: no-step trials (30%) and step trials (70%).

In no-step trials, following fixation for a variable duration (~300 ms), a peripheral green target appeared in one of six equally spaced peripheral locations (see below) on an imaginary circle of radius 12°. The appearance of the target was the go cue for the monkey to make a saccade to the target as soon as possible. The reaction time (RT) for the G saccade in the no-step trials was defined as the time from the appearance of the target until the saccade onset (Fig. 1*A* and *SI Appendix*, Fig. S1*D*).

In the step trials, after the fixation point appearance, two targets appeared sequentially (initial: green; final: red), with a variable time delay between them (17, 83 , or 150 ms), referred to as the "target step delay" (*SI Appendix*, Fig. S1*B*). We flashed the second target almost always in the

hemifield diametrically opposite the hemifield of the first target position. A correct response in the step trials entailed making a sequence of two goal-directed saccades: from the fixation point to the first target (G1 saccade), and from the first target to the second target (G2 saccade). Correct responses were rewarded with a liquid reward. In step trials, the reaction time for the G1 saccade was defined as the time from the appearance of the first target until the G1-saccade onset (Fig. 1*B* and *SI Appendix*, Fig. S1*D*). The reaction time for the G2 saccade was defined as the time from the appearance of the second target until the G2-saccade onset (Fig. 1*B* and *SI Appendix*, Fig. S1*D*).

While the MGS task had eight possible target locations, a restricted set of target positions and steps was used during neurophysiological recording sessions to maximize collection of relevant follow task data. After RF identification using the MGS task, typically three target locations centered on the RF were considered to be "in-RF" directions and the three directions diametrically opposite them were considered to be out of the response field or "in-aRF" directions. The targets in no-step trials and the first targets in step trials could appear in any one of the six RF and aRF directions. However, the second target in step trials could only appear in one of the three directions diametrically opposite the direction of the first target. Thus, the second target could either step into or out of the response field but never within or adjacent to it. Following successful completion of the task, monkeys made no or several non–goal-directed saccades until they finally made a saccade back to the center of the screen to initiate the next trial. Trials with artifacts including eye blinks and saccades with reaction times less than 100 ms on both tasks were removed prior to further data analysis. Throughout the experiment, the room in which the monkeys were was completely dark with no visual features at the fixation spot until after the saccade had been completed in each trial.

Data Collection. TEMPO/VIDEOSYNC software (Reflective Computing) was used simultaneously with the Cerebus Data Acquisition System (Blackrock Microsystems) for data collection. Eye positions were sampled with a monocular infrared pupil tracker (ISCAN), interfaced with TEMPO software in real time. The stimuli were presented on a calibrated Sony Bravia liquid-crystal display monitor (21 inch; 60-Hz refresh rate) placed 57 cm in front of the monkey. Raw neural signals from 84 neurons were collected using single tungsten microelectrodes (FHC; impedance 2 to 4 MΩ) from the FEF on the right hemisphere through a permanently implanted recording chamber (Crist Instrument). These raw neural signals were acquired at 30,000 Hz and subsampled to 1,000 Hz, low-pass–filtered (from 0 to 150 Hz) to obtain LFP and high-pass–filtered (from 300 to 3,000 Hz) to obtain spikes.

Data Analysis.

Visuomotor index. We classified the recorded FEF neurons as visual, vismov, or movement neurons (*SI Appendix*, Fig. S2) based on their relative visual and movement-related activities in a memory-guided saccade task. The visuomotor index was calculated as (VA − MA)/(VA + MA), where VA is the average neural activity 50 to 200 ms from the target onset and MA is the average activity 100 to 0 ms before saccade onset. The visuomotor index can range from +1 to −1. Neurons with a visuomotor index in the range of [0.3, 1) were taken as visual neurons (n = 12), [−0.3, 0.3] were taken as vismov neurons (n = 34), and (−1, −0.3] were taken as movement neurons (n = 38).

Mean-matched Fano factor. The Fano factor is defined as the variance in neural activity across trials divided by the mean firing rate. Thus, it can be susceptible to within-trial changes in firing rate due to its mathematical definition. To circumvent this problem, we calculated the Fano factor on a mean-matched firing rate. Details of this algorithm are described elsewhere (9). Briefly, we calculated the mean spike count and variance for each neuron, for each direction (RF or aRF), and for each condition (type of saccade) in a 50-ms time interval, shifted by 25 ms. Since we wanted to have the same distribution of mean firing rates (but not variances) at each time window, we pooled all neurons together and compared the distributions of means (of firing rates) at each time window and then selected the greatest common distribution. We then subsampled neurons at each time window to match that distribution and then plotted the ratio of the variance to the mean for those subsets to get the mean-matched Fano factor. The algorithm preserved 40, 41, 37, and 43% of data for G, G1, nG, and G2 saccades, respectively.

Matching intersaccade intervals. The monkeys were required to fixate on the final target, in either trial type, for 200 ms. On average, the monkeys initiated the first nG saccade 475 ms after the G saccade in the no-step trials and initiated the G2 saccade 240 ms after the G1 saccade in the step trials (*SI Appendix*, Fig. S1*E*). To match the intersaccade intervals between the two types of trials, we restricted all our analyses to only pairs of consecutive saccades whose saccade onset times were at least 300 ms apart (see *SI Appendix*, Fig. S1*E* for illustration). The reaction times for the G and G1 saccades were similar individually for both monkeys while the reaction time for G2 saccades was much longer, as expected (*SI Appendix*, Fig. S1*D*).

This step was also necessary to avoid measurement complications due to parallel processing of saccades that are temporally close (intersaccade interval [ISI] < 300 ms) (14, 27). This is further illustrated in *SI Appendix*, Fig. S8. Clearly, the firing rate, FF, beta, and SPS between the two conditions around G2 were not different between the short- and long-ISI trials. Importantly, there was a decrease in FF and beta around the G2 saccade, as was observed for all goal-directed movements, in general. However, for both measures, we observed that the associated decreases began much earlier. These data are consistent with previous reports (14, 28) that indicate that at lower target step delays, associated with short ISIs (<300 ms), there is parallel processing of two saccades. Consequently, for the short-ISI condition, the FF and beta show a shallow W-shaped activity due to closely spaced responses to plans 1 and 2. This is especially visible in beta activity because much of the time domain information needs to be sacrificed to obtain precise frequency domain information due to the time–frequency trade-off. SPS could not be calculated for short-ISI conditions due to parallel processing. Thus, the presence of concurrent activity makes quantification of G2-related activity without contamination from G1-related activity problematic.

Saccade Kinematics Matching. We matched G saccades to G1 saccades and nG saccades to G2 saccades in terms of both saccade amplitude and peak velocity, using the k-nearest neighbor approach (29) (where k = 3; *SI Appendix*, Fig. S6). For instance, to match G saccades to G1 saccades, it suffices to find a subpopulation of G saccades that are a subset of G1 saccades in terms of amplitude and peak velocity. Therefore, for each G saccade, we calculated its saccade amplitude and peak velocity and drew a tolerance window around it: ±1° amplitude and ±25°/s velocity. If we found at least three G1 saccades within every such G saccade's tolerance window, then we classified that G saccade as being "matched" with G1. We repeated this process to match nG saccades with G2 saccades. In this way, 99.34% of G saccades were matched with G1 saccades (*SI Appendix*, Fig. S6 *A*, *Bottom Right*) but only 46.43% of nG saccades were matched with G2 saccades (*SI Appendix*, Fig. S6 *C*, *Bottom Right*). The remaining saccades were discarded in each case for further calculations of G or nG saccade-related activity except for the analyses in *SI Appendix*, Fig. S6. To further validate our result, we divided the nG-saccade velocities into three groups, short, medium, and long, and calculated the FF in each group for nG and G2 saccades (*SI Appendix*, Fig. S7).

Saccade Plan Specification Time. We defined the SPS time as the first time point when the signals in at least one of the eight saccade directions significantly differed from each other (4). To calculate SPS for each neuron, we averaged single neuronal activity (sigma = 10 ms) for each direction, sorted on RF, and then averaged them across the population. Then, we computed a p-ANOVA among the average population neural activities in eight directions in 1-ms bins from −400 to 200 ms from saccade onset. This calculation gave a P value for every millisecond of the data indicating the probability that the signal did not significantly differ among the eight directions. We calculated the first time point when the P value fell below 0.05 backward from the saccade onset and remained below 0.05 continuously for the next 60 ms to measure SPS (Fig. 3).

Spectrum and Spectrogram. LFP spectra were computed using mtspectrumc and spectrograms were constructed using mtspecgramc functions in Chronux using the multitaper algorithm (30). We used five tapers for each analysis and a window length of 300 ms with step size 30 ms to calculate the spectrogram. Spectrograms calculated in this way were normalized by subtracting the log of each value from the log of the baseline power spectrum, in the respective frequency ranges, to get the change in power for each frequency component with respect to time. The frequency range from 13 to 30 Hz was taken as the beta band for all further analyses (4).

Statistics. To check if two independent distributions were significantly different from each other, we first performed a two-sided goodness-of-fit Lilliefors test to test for the normality and then used an appropriate t test or else a nonparametric Wilcoxon rank-sum test. All values in this study, unless stated otherwise, are mean ± SEM.

Data Availability. Physiological data reported in this article have been deposited at https://data.mendeley.com/datasets/nhhmrw79z9/1 (31).

ACKNOWLEDGMENTS. This work was supported by a Department of Biotechnology-Indian Institute of Science partnership program grant and institutional support from the Ministry of Human Resource Development. This work was also supported by R21 EY-020631, 1 R01 NS113078-01, and

P30 EY-019007 (to M.E.G., principal investigator) and the Dana Foundation through the David Mahoney Chair in Brain and Behavior Research, Columbia University. J.D.S. was supported by Robin and Richard Patton through the E. Bronson Ingram Chair in Neuroscience.

1. C. J. Bruce, M. E. Goldberg, Primate frontal eye fields. I. Single neurons discharging before saccades. *J. Neurophysiol.* **53**, 603–635 (1985).
2. E. Bizzi, Discharge of frontal eye field neurons during saccadic and following eye movements in unanesthetized monkeys. *Exp. Brain Res.* **6**, 69–80 (1968).
3. B. A. Purcell, R. P. Heitz, J. Y. Cohen, J. D. Schall, Response variability of frontal eye field neurons modulates with sensory input and saccade preparation but not visual search salience. *J. Neurophysiol.* **108**, 2737–2750 (2012).
4. N. Sendhilnathan, D. Basu, A. Murthy, Simultaneous analysis of the LFP and spiking activity reveals essential components of a visuomotor transformation in the frontal eye field. *Proc. Natl. Acad. Sci. U.S.A.* **114**, 6370–6375 (2017).
5. B. Pesaran, J. S. Pezaris, M. Sahani, P. P. Mitra, R. A. Andersen, Temporal structure in neuronal activity during working memory in macaque parietal cortex. *Nat. Neurosci.* **5**, 805–811 (2002).
6. J. F. Mitchell, K. A. Sundberg, J. H. Reynolds, Differential attention-dependent response modulation across cell classes in macaque visual area V4. *Neuron* **55**, 131–141 (2007).
7. N. Sendhilnathan, D. Basu, A. Murthy, Assessing within-trial and across-trial neural variability in macaque frontal eye fields and their relation to behaviour. *Eur. J. Neurosci.* **52**, 4267–4282 (2020).
8. M. M. Churchland, B. M. Yu, S. I. Ryu, G. Santhanam, K. V. Shenoy, Neural variability in premotor cortex provides a signature of motor preparation. *J. Neurosci.* **26**, 3697–3712 (2006).
9. M. M. Churchland *et al*., Stimulus onset quenches neural variability: A widespread cortical phenomenon. *Nat. Neurosci.* **13**, 369–378 (2010).
10. A. L. Falkner, M. E. Goldberg, B. S. Krishna, Spatial representation and cognitive modulation of response variability in the lateral intraparietal area priority map. *J. Neurosci.* **33**, 16117–16130 (2013).
11. A. Pogosyan, L. D. Gaynor, A. Eusebio, P. Brown, Boosting cortical activity at beta-band frequencies slows movement in humans. *Curr. Biol.* **19**, 1637–1641 (2009).
12. A. Stancák Jr, G. Pfurtscheller, Event-related desynchronisation of central beta-rhythms during brisk and slow self-paced finger movements of dominant and non-dominant hand. *Brain Res. Cogn. Brain Res.* **4**, 171–183 (1996).
13. A. K. Engel, P. Fries, Beta-band oscillations—Signalling the status quo? *Curr. Opin. Neurobiol.* **20**, 156–165 (2010).
14. D. Basu, A. Murthy, Parallel programming of saccades in the macaque frontal eye field: Are sequential motor plans coactivated? *J. Neurophysiol.* **123**, 107–119 (2020).
15. M. H. Chang, K. M. Armstrong, T. Moore, Dissociation of response variability from firing rate effects in frontal eye field neurons during visual stimulation, working memory, and attention. *J. Neurosci.* **32**, 2204–2216 (2012).
16. J. F. Mitchell, K. A. Sundberg, J. H. Reynolds, Spatial attention decorrelates intrinsic activity fluctuations in macaque area V4. *Neuron* **63**, 879–888 (2009).
17. M. C. Bushnell, M. E. Goldberg, D. L. Robinson, Behavioral enhancement of visual responses in monkey cerebral cortex. I. Modulation in posterior parietal cortex related to selective visual attention. *J. Neurophysiol.* **46**, 755–772 (1981).
18. K. G. Thompson, K. L. Biscoe, T. R. Sato, Neuronal basis of covert spatial attention in the frontal eye field. *J. Neurosci.* **25**, 9479–9487 (2005).
19. M. R. Cohen, J. H. R. Maunsell, Attention improves performance primarily by reducing interneuronal correlations. *Nat. Neurosci.* **12**, 1594–1600 (2009).
20. S. Waldert *et al*., Hand movement direction decoded from MEG and EEG. *J. Neurosci.* **28**, 1000–1008 (2008).
21. F. Cassim *et al*., Brief and sustained movements: Differences in event-related (de) synchronization (ERD/ERS) patterns. *Clin. Neurophysiol.* **111**, 2032–2039 (2000).
22. C. C. Chen *et al*., Excessive synchronization of basal ganglia neurons at 20 Hz slows movement in Parkinson's disease. *Exp. Neurol.* **205**, 214–221 (2007).
23. J. P. Lieb, T. L. Babb, J. Engel Jr, Quantitative comparison of cell loss and thiopental-induced EEG changes in human epileptic hippocampus. *Epilepsia* **30**, 147–156 (1989).
24. R. M. Dasheiff, W. A. Kofke, Evaluation of the thiopental test in epilepsy surgery patients. *Epilepsy Res.* **15**, 253–258 (1993).
25. O. Jensen *et al*., On the human sensorimotor-cortex beta rhythm: Sources and modeling. *Neuroimage* **26**, 347–355 (2005).
26. R. H. Wurtz, M. E. Goldberg, Activity of superior colliculus in behaving monkey. 3. Cells discharging before eye movements. *J. Neurophysiol.* **35**, 575–586 (1972).
27. D. Basu, N. Sendhilnathan, A. Murthy, Capacity sharing between concurrent movement plans in the frontal eye field during the planning of sequential saccades. *bioRxiv* [Preprint] (2020). https://doi.org/10.1101/2020.12.04.411454.
28. S. Ray, N. Bhutani, A. Murthy, Mutual inhibition and capacity sharing during parallel preparation of serial eye movements. *J. Vis.* **12**, 17 (2012).
29. T. Cover, P. Hart, Nearest neighbor pattern classification. *IEEE Trans. Inf. Theory* **13**, 21–27 (1967).
30. D. J. Thomson, Spectrum estimation and harmonic analysis. *Proc. IEEE* **70**, 1055–1096 (1982).
31. N. Sendhilnathan, Neural correlates of goal-directed and non-goal-directed movements, Mendeley Data. https://data.mendeley.com/datasets/nhhmrw79z9/1. Deposited 22 January 2021.